Values of the strength coefficient σ_0 and the hardening exponent n for a number of steels are given in Table 1. These data are taken from an extensive list compiled by Marin.[8] Descriptions of methods for obtaining the values of σ_0 and n from tensile test data are given in Refs. 7 and 9. With the exception of type-304 stainless, a highly ductile austentitic steel, the values of n given in Table 1 lie in the range $0 \leq n \leq 0.3$. It can be shown[9] that the strain at maximum load in a tensile test is equal to n for a material with a stress-strain relation of the form $\sigma = \sigma_0 \epsilon^n$. Hence, high-strength steels, since they have little ductility, have the smallest values of n.

References

[1] Salmon, M. A., "Plastic instability of cylindrical shells with rigid end closures," Am. Soc. Mech. Engrs. 63-APM-13 (June 24, 1963).

[2] Weil, N. A. and Newmark, N. M., "Large plastic deformations of circular membranes," J. Appl. Mech. 4, 533–538 (1955).

[3] Grigoriev, A. S., "State of stress in cylindrical membrane shells at large deformations," Prikl. Math. Mech. 21, 827–832 (1957).

[4] Grigoriev, A. S., "Equilibrium of a membrane of revolution at large deformations," Prikl. Math. Mech. 25, 1083–1090 (1961).

[5] Weil, N. A., "An approximate solution for the bursting of thin-walled cylinders," Intern. J. Mech. Sci. (to be published).

[6] Hill, R., *The Mathematical Theory of Plasticity* (Oxford University Press, London, 1956), Chap. II.

[7] Svenson, N. L., "The bursting pressure of cylindrical and spherical vessels," J. Appl. Mech. 25, 89–96 (1958).

[8] Marin, J. and Weng, T., "Strength of thick walled cylindrical pressure vessels," Dept. Eng. Mech., Pennsylvania State Univ. (1961).

[9] Marin, J., *Mechanical Behavior of Engineering Materials* (Prentice Hall Inc., Englewood Cliffs, N. J., 1962), Chap. 1.

SEPTEMBER 1963 AIAA JOURNAL VOL. 1, NO. 9

Bending Vibrations of a Circular Cylindrical Shell with an Internal Liquid Having a Free Surface

ULRIC S. LINDHOLM,* WEN-HWA CHU,* DANIEL D. KANA,† AND H. NORMAN ABRAMSON‡
Southwest Research Institute, San Antonio, Texas

Resonant bending frequencies and mode shapes were determined experimentally for a thin circular cylindrical shell containing an internal liquid with a free surface. The measured increase in frequency between uncapped and capped partially filled tanks of two different end conditions are generally in agreement with theoretical predictions. Differences between theory and experiment are attributed primarily to variations of actual mode shapes from those assumed in the theory. This is true for both cantilever and pin-ended tanks, with the latter being even more complicated by a strong dependence of mode shape on liquid depth. Significant coupling occurred between bending and breathing shell responses, becoming increasingly important with decreasing tank-fineness ratio.

Introduction

THIS paper represents a continuation of the authors' studies of the dynamic interaction of a flexible tank with an internally contained liquid. A previous paper[1] dealt with the effect of the internal liquid column on the *breathing* vibrations of the tank wall. The present study is concerned with the coupled tank-liquid system resonant *bending* frequency for thin circular cylindrical shells and, particularly, with the effect of the liquid free surface motion on the coupled bending resonance. The studies were initiated using uniform shells, where the coupled resonant frequencies were at least an order of magnitude greater than the uncoupled liquid free surface resonances. In subsequent work a theoretical investigation was made of the behavior of tanks with added tip masses, in order to establish the influence of coupling when the bending resonance is in the neighborhood of the lower sloshing resonances. This latter condition more nearly approximates the condition in actual launch vehicles.

Presented at the IAS 31st Annual Meeting, New York, January 21–23, 1963; revision received July 8, 1963. The results reported in this paper were obtained during the course of research sponsored by NASA under Contract NASw-146. The authors are indebted to the Southwest Research Institute's Computations Laboratory for performing the theoretical calculations and to Gilbert F. Rivera for preparing the illustrations.

* Senior Research Engineer, Department of Mechanical Sciences.

† Research Engineer, Department of Mechanical Sciences.

‡ Director, Department of Mechanical Sciences. Associate Fellow Member AIAA.

Available theoretical analyses show that the presence of the liquid free surface, with its associated sloshing modes, may shift the fundamental bending frequency of the liquid-flexible tank system by an appreciable amount over that which would occur if the free surface motion were not present. Problems of flexible tank dynamics are therefore important from the point of view of the missile designer, who must have precise knowledge of the system resonant frequencies in order that unduly large structural stresses are not created and also that the structural resonances do not occur in the neighborhood of the missile control system frequencies and thus produce serious coupling effects. The present program was initiated in order to verify experimentally the existing analyses of the free bending vibrations of a tank, partially filled with a liquid.

Miles[2] has derived the frequency equation for the liquid-filled circular cylindrical tank including free liquid surface effects using the Lagrangian energy approach. Particular results cited by Miles in his paper give increases in the fundamental resonant bending frequency resulting from liquid sloshing of 5% and 27% for full cantilever and freely supported tanks of fineness ratio equal to one. This indicates that in order to determine resonant frequencies accurately it is necessary to take into account the free surface boundary condition in determining the total apparent mass of the liquid. The free surface coupling always results in an *increase* in the resonant bending frequency over that for the capped tank.§

§ Here, and throughout this paper, a capped tank refers to one in which the liquid sloshing motion is suppressed, i.e., the free surface remains a plane surface normal to the tank generator.

Several other investigators have considered the problem of liquid-flexible tank interactions. In addition to other related problems, Reissner[3] indicates two methods of solution for the flexible tank containing a liquid with a free surface. The first is to formulate the problem as an integral equation to be solved for the wall displacement. The resulting homogeneous integral equation then is solvable approximately by collocation methods. The second formulation indicated is a variational treatment using the principle of minimum complementary energy. However, specific examples for the bending tank are not worked out in his paper. Rabinovich[4] uses an integro-differential approach to the partially filled tank problem. The liquid potential function is derived by using a Lagrange-Cauchy integral, from which expressions for the hydrodynamic and hydrostatic forces acting on the tank walls are obtained. These expressions then are introduced into the differential equation for the oscillations of a thin-walled elastic bar. Characteristic frequencies of the resulting integro-differential equation then can be solved by Galerkin's method.

The problem of forced bending vibration at low frequencies, in the neighborhood of the resonant sloshing frequencies, has been studied by Bauer[5] in a manner similar to that for translation or rotation of a rigid tank. The problem is solved for the liquid potential, the shape of the free surface, the total force and moment of the liquid, and the pressure and velocity distribution. The effect of damping in the system is covered by Bauer in a separate report.[6]

Since the Lagrangian analysis as applied by Miles directly yields the frequency determinant for an assumed bending mode shape, this method was used for correlation with experimentally-determined resonant frequencies. Solutions are obtained for the resonant bending frequencies of partially full cantilever and simply supported circular cylindrical tanks of varying fineness ratios. The capped and uncapped resonant frequencies then are compared both analytically and experimentally for a number of tanks.

Theoretical Analyses

Consider a uniform thin wall circular cylindrical tank of length l, liquid depth $2b$, and radius a, as shown in Fig. 1. Following Miles, the equations of motion may be determined from a Lagrangian formulation of the problem taking the kinetic energy in the form

$$T = \frac{1}{2}\sum_i\sum_j m_{ij}\dot{q}_i\dot{q}_j$$

and the potential energy as

$$V = \frac{1}{2}\sum_i\sum_j k_{ij}q_iq_j$$

where the q_i are generalized coordinates corresponding to translation, rotation, bending, and sloshing motion of the coupled system. The derivation of the kinetic and potential energy coefficients m_{ij} and k_{ij} for the system under consideration is given in Miles' paper, and, therefore, the details will not be repeated here. The coefficients for coupled bending-liquid free surface oscillations are given in Appendix A, however, for reference. These coefficients are derived from a velocity potential so that nonviscous, irrotational flow is assumed.

The equations of motion, obtained from the substitution of the energy expressions into Lagrange's equations, for bending and liquid free-surface motion only, are

$$(\bar{m}_e + \bar{m}_{3,3})\ddot{q}_3 + \sum_1^\infty \bar{m}_{3,s+3}\,\ddot{q}_{s+3} + (\bar{m}_e\omega_e^2 + \bar{k}_{3,3})q_3 + \sum_1^\infty \bar{k}_{3,s+3}\,q_{s+3} = 0 \quad (1a)$$

$$\bar{m}_{3,s+3}\,\ddot{q}_3 + \bar{m}_{s+3,s+3}\,\ddot{q}_{s+3} + \bar{k}_{3,s+3}\,q_3 + \bar{k}_{s+3,s+3}\,q_{s+3} = 0 \quad (1b)$$
$$s = 1,2,3\ldots$$

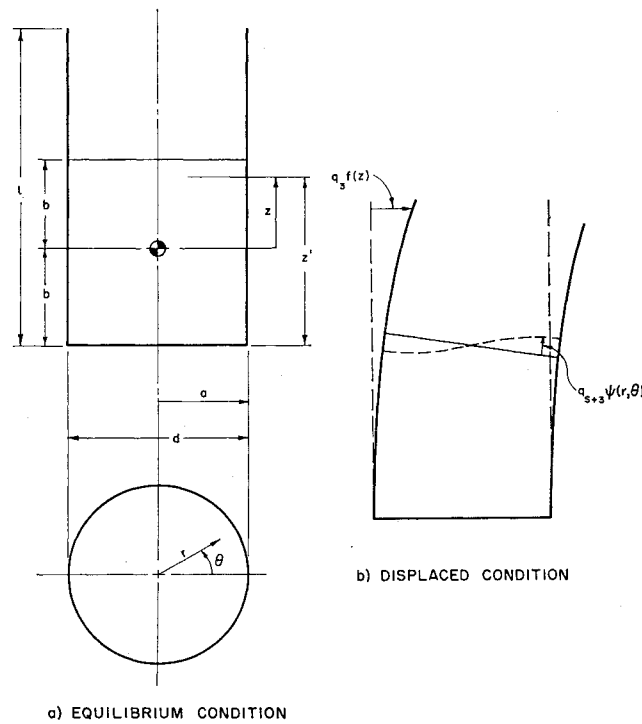

Fig. 1 Coordinate system for the bending tank containing an internal liquid.

The frequency equation obtained from Eqs. (1a, b), by assuming periodic motion, is

$$\omega^2 - \omega_3^2 - \sum_{s=1}^{\infty} \alpha_{3s}\frac{(\omega^2 - \Omega_{3s})^2}{\omega^2 - \omega^2_{s+3}} = 0 \quad (2)$$

The subscripts 3 and $s+3$ correspond to the generalized displacements, $q_3(t)f(z)$ denoting bending displacement and $q_{s+3}(t)\psi(r,\theta)$ denoting displacement of the free liquid surface from a plane normal to the generator of the cylinder (see Fig. 1). In Eqs. (1) and (2) the following notation is used:

$$\omega_3 = \left(\frac{\bar{m}_e\omega_e^2 + \bar{k}_{3,3}}{\bar{m}_e + \bar{m}_{3,3}}\right)^{1/2} = \text{uncoupled bending frequency}$$

$$\omega_{s+3} = \left(\frac{\bar{k}_{s+3,s+3}}{\bar{m}_{s+3,s+3}}\right)^{1/2} = \text{uncoupled sloshing frequencies}$$

$$\Omega_{3s} = \frac{\bar{k}_{3,s+3}}{\bar{m}_{3,s+3}} = \text{coupling coefficients}$$

$$\alpha_{3s} = \frac{\bar{m}^2_{3,s+3}}{\bar{m}_{s+3,s+3}(\bar{m}_e + \bar{m}_{3,3})} = \text{coupling coefficients}$$

$\bar{m}_e$ and ω_e are the effective empty tank mass and resonant bending frequency, respectively. The bars over the coefficients indicate normalization by the total liquid mass.

The frequency equation has an infinite number of roots $\omega = \omega_n$. The root in the neighborhood of ω_3, the uncoupled bending frequency, is of primary interest. A considerably simplified expression may be obtained for this root if the coupled bending frequency ω is large compared with the sloshing frequencies ω_{s+3} and the coupling coefficient Ω_{3s}. This will be the case for the uniform cylindrical shell, since ω is large for this case, and at these high frequencies the coupling between bending and sloshing mainly is inertial. By neglecting Ω_{3s} and ω_{s+3} in comparison with ω, the simplified frequency equation

$$\omega^2 = \omega_3^2\left[1 - \sum_{s=1}^{\infty}\alpha_{3s}\right]^{-1} \quad (3)$$

is obtained. The difference between the coupled and un-

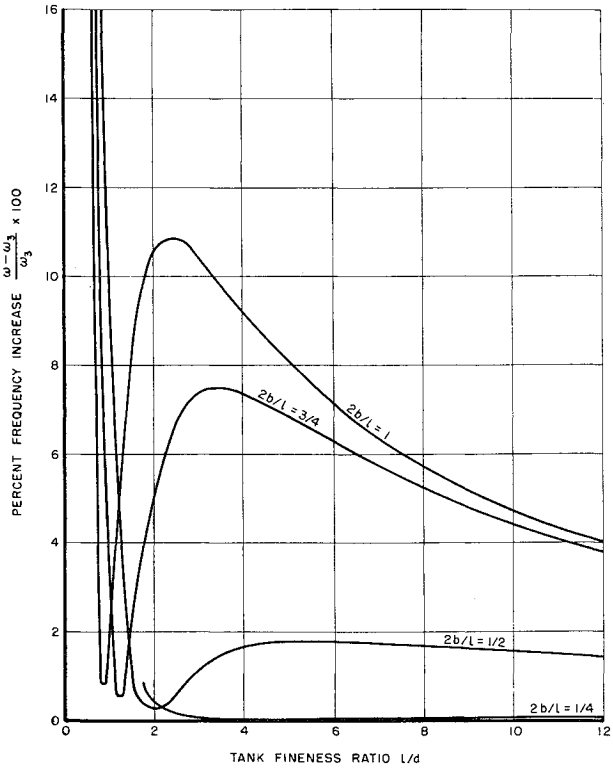

Fig. 2 Percent increase in resonant bending frequency as a result of the coupling with liquid free surface motions for cantilever tanks of varying fineness ratio l/d and fractional liquid depth.

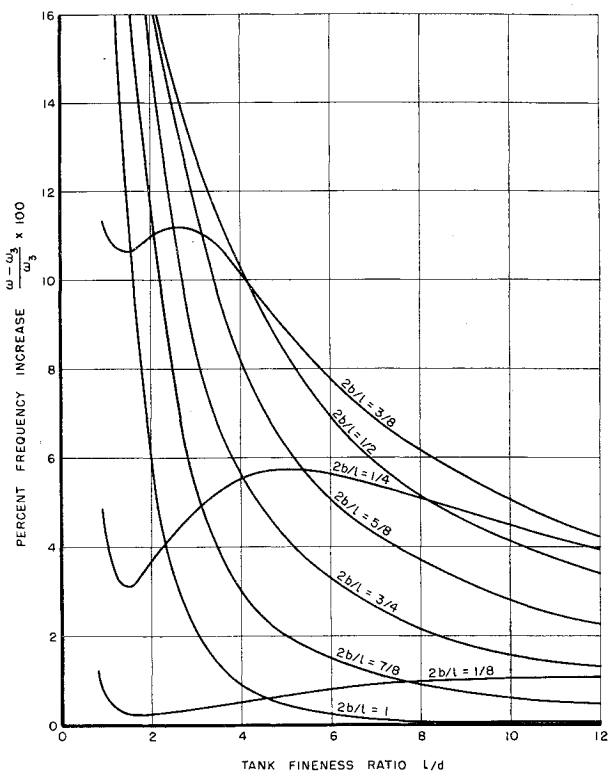

Fig. 3 Percent increase in resonant bending frequency as a result of the coupling with liquid free surface motions for pin-ended tanks of varying fineness ratio l/d and fractional liquid depth.

coupled bending frequencies thus is determined by the coefficients α_{3s}. The uncoupled inertia coefficients, $\bar{m}_{3,3}$, $\bar{m}_{s+3,s+3}$, and $\bar{m}_e$, always are positive. The inertia coupling coefficient $\bar{m}_{3,s+3}$ may be either positive, negative, or zero, depending upon the ratio b/a. When $\bar{m}_{3,s+3} = 0$, it follows that $\alpha_{3s} = 0$, causing a sharp minimum in coupling for certain tank configurations (the coupling need not actually become zero because of the summation over s and the presence of the small potential coupling $\bar{k}_{3,s+3}$). This minimum in coupling is noted particularly in the results for the cantilever tank near $b/a = 1$. This situation is analogous to the inertially coupled bending and torsional vibrations of a beam, in which case the uncoupling occurs when the shear center of a beam coincides with its centroid. For $\bar{m}_{3,s+3} \neq 0$, the factor $[1 - \Sigma\alpha_{3s}]^{-1}$ is always greater than unity, thus always yielding an increase in the coupled bending frequency due to the presence of the free liquid surface.

In the forementioned analysis, as in the paper of Miles, attention was centered on the root ω_n of the frequency equation near the bending frequency ω_3 of the capped tank. There are other roots of this equation, however, which correspond to and lie near the liquid sloshing frequencies ω_{s+3}, i.e., the coupling between the bending and sloshing also changes the resonant sloshing frequencies from their uncoupled or rigid tank values. If only the root of the frequency equation in the neighborhood of ω_{s+3} is looked at, this equation can be written, by neglecting the summation, as

$$\omega^2 - {\omega_3}^2 - \alpha_{3s}\frac{(\omega^2 - \Omega_{3s})^2}{\omega^2 - {\omega^2}_{s+3}} = 0 \tag{4}$$

Let $\Delta = \omega^2 - {\omega^2}_{s+3}$, the difference between the uncoupled sloshing frequency and the root of the coupled frequency equation near ω_{s+3}. With a little manipulation, the following quadratic equation for Δ is obtained:

$$(1 - \alpha_{3s})\Delta^2 - [{\omega_3}^2 - {\omega^2}_{s+3} - 2\alpha_{3s}(\Omega_{3s} - {\omega^2}_{s+3})]\Delta - \alpha_{3s}(\Omega_{3s} - {\omega^2}_{s+3})^2 = 0 \tag{5}$$

Solvin for Δg yields

$$\Delta = \frac{1}{2(1 - \alpha_{3s})}\{{\omega_3}^2 - {\omega^2}_{s+3} - 2\alpha_{3s}(\Omega_{3s} - {\omega^2}_{s+3}) - ([{\omega_3}^2 - {\omega^2}_{s+3} - 2\alpha_{3s}(\Omega_{3s} - {\omega^2}_{s+3})]^2 + 4(1 - \alpha_{3s})\alpha_{3s}(\Omega_{3s} - {\omega^2}_{s+3})^2)^{1/2}\}$$

$$\cong \frac{1}{2(1 - \alpha_{3s})}\left\{{\omega_3}^2 - {\omega^2}_{s+3} - 2\alpha_{3s}(\Omega_{3s} - {\omega^2}_{s+3}) - [{\omega_3}^2 - {\omega^2}_{s+3} - 2\alpha_{3s}(\Omega_{3s} - {\omega^2}_{s+3})] \times \left[1 + \frac{2(1 - \alpha_{3s})\alpha_{3s}(\Omega_{3s} - {\omega^2}_{s+3})^2}{[{\omega_3}^2 - {\omega^2}_{s+3} - 2\alpha_{3s}(\Omega_{3s} - {\omega^2}_{s+3})]^2} + \cdots\right]\right\}$$

$$\cong -\frac{\alpha_{3s}(\Omega_{3s} - {\omega^2}_{s+3})^2}{{\omega_3}^2 - {\omega^2}_{s+3} - 2\alpha_{3s}(\Omega_{3s} - {\omega^2}_{s+3})} \tag{6}$$

The forementioned approximation involves neglecting second- and higher-order terms in the expansion of the radical of the first expression. This will be valid for $\omega_{s+3} \ll \omega_3$. If it is noted also that $\alpha_{3s} < 1$ and $\Omega_{3s} \ll \omega$, a further approximation can be made giving

$$\Delta = \omega^2 - {\omega^2}_{s+3} \cong -\frac{\alpha_{3s}(\Omega_{3s} - {\omega^2}_{s+3})^2}{{\omega_3}^2} \tag{7}$$

Since α_{3s} is always a positive quantity, the coupled sloshing resonances will be always less than the uncoupled values. Under the assumption of ω_3 large, the difference will be small.

Equation (3) is solved for the particular cases of uniform cantilever and pin-ended tanks with the liquid at varying partial depths $2b/l$. The integrated expressions for the relevant m_{ij} and k_{ij} for these two end conditions and assumed mode shapes are given in Appendix B. The expressions for the cantilever tank are the same as those given by Miles with $l = 2b$ (full tank), except for an additional term in $\bar{m}_e$ to include the effect of the rotary inertia of the tank. Figures 2 and 3 show the results for these two tank configurations

plotted as the percent increase in bending frequency due to coupling $[(\omega - \omega_3)/\omega_3] \times 100$ vs tank-fineness ratio l/d for varying partial depths $2b/l$. These curves may be affected appreciably by the assumed bending mode shape, which in these analyses involved a parabolic mode shape for the cantilever tank and a sinusoidal mode shape for the pin-ended tank. The effect of variation from these assumed mode shapes is demonstrated and discussed in the section of this paper dealing with the experimental results.

The curves in Figs. 2 and 3 are for the special case of a uniform shell where $\omega_3 \gg \omega_{s+3}$. In order to determine the effect of coupling on the resonant frequencies of the system when ω_3 and ω_{s+3} are of the same order of magnitude, the exact frequency equation (2) was solved for a cantilever tank with an added tip mass. The tip mass was added in order to lower the bending resonance. Analytically, this involved only a slight modification of the empty tank inertia coefficient $\bar{m}_e$ but required considerably more effort in solving for the eigenvalues of the frequency determinant of the set of Eqs. (1a) and (1b). In the analysis, six modes, one bending and five sloshing, were used.

The results of this analysis showed that the addition of mass to the vibrating system, although lowering the resonant bending frequency, also reduces the effect of the sloshing mass on the response of the entire system. For the cantilever tank, the addition of a tip mass of 10 times the empty tank mass reduced the maximum frequency increase of approximately 11% as shown in Fig. 2 to less than 1.5%. Further increases in tip mass reduce the influence of the free surface on resonant bending frequency still further. It would appear, therefore, that consideration of the free surface boundary condition will only be significant in those cases where the sloshing mass is an appreciable portion of the total vibrating mass, as in the bending of relatively low fineness ratio, uniform shells. For large missile structures where the total bending mass is large, the liquid sloshing mass can be neglected in the calculation of overall bending resonant frequencies without significant error.

The solution for all six roots of the coupled frequency equations showed also that the resonant sloshing frequencies did not change appreciably from their uncoupled values. Thus, rigid tank sloshing frequencies are adequate for use in the bending tank.

Experimental Apparatus and Procedures

The overall apparatus and instrumentation used to obtain the coupled liquid-tank fundamental bending frequency data from the various tanks examined is essentially the same as that used in previous studies of breathing vibrations of shells containing a liquid.[1] Briefly, the apparatus consists of three components: the support fixture, the excitation system, and the sensing system. The support fixture provides a mount for thin steel cylindrical tanks, including the various desired end conditions. In addition, this fixture provides support for portions of the other two systems. An electromagnetic coil is mounted on the test fixture so that its core is very close to, but not in contact with, the tank. Excitation is provided by driving the coil with an oscillator through a 200-w-power amplifier. The lateral displacement of the tank is monitored by two noncontacting inductance-type displacement transducers mounted on the test fixture in close proximity to the tank. One probe is fixed for a reference displacement, whereas the other can be moved axially and circumferentially around the cylinder so that radial displacement at any location on the tank can be monitored. Relative displacement is read on an oscilloscope whereas frequency is determined accurately on an electronic counter.

A slight modification to the test fixture was necessary to provide a capping device to suppress the free surface of the liquid inside the shell. Figure 4 shows a simplified sketch of the test fixture with a pin-ended tank mounted in it, and the capping device mounted and extending down into the tank. The cap is made of clear plastic and machined to a 0.015-in. clearance on the inside diameter of the tank. The cap also contains several small holes to prevent air pockets from forming as the cap is lowered onto the liquid surface. Two $\frac{1}{4}$-in. rods allow the cap to be adjusted to the desired elevation. It was found necessary to secure a lead weight to the cap to provide a very low resonant frequency in the capping device, since induced vibrations in this cap could produce severe error in the measured data.

The thin circular cylindrical tanks were machined from 4130 steel seamless tubing. Three different length tanks, 15.95 in., 9.20 in., and 5.20 in., were each tested in the cantilever and pin-ended support condition. The effective lengths in the cantilevered condition were 1 in. less than in the pin-ended condition because of the clamping at one end. All tanks were 2.970-in. mean diameter and 0.010-in. wall thickness.

The dimensions of these tanks were chosen to provide experimental correlation in a range of l/d ratios. Unfortunately, uniform liquid filled shells of these sizes pose a severe problem by virtue of their possessing many breathing resonant frequencies, each of which has its own variation with liquid depth.[1] Some of these breathing resonances occur near the fundamental bending frequency and have displacement responses that are far more prominent than that of the bending response. In order to suppress the more prominent breathing responses and still maintain a circular cross section for bending, it was necessary to secure thin stiffener rings around the outside of the tanks. These $\frac{1}{8}$-in. wide by $\frac{1}{16}$-in. thick evenly spaced aluminum rings were cemented to the outside of the tanks. It obviously was desirable to use as few rings as possible, but it still was found necessary to use from three to five rings, depending on the tank length. Even then it was not possible to suppress the most prominent breathing modes, and it was impossible to obtain bending data at some liquid depths where these coupled with the bending. In fact, it was impossible to get any bending information from the 5.20-in.-long tank in any condition.

The procedure followed was to determine the resonant bending frequency at a given liquid depth with the cap just in contact with the free surface and with the cap removed. This was repeated several times at each depth to obtain average frequency values. The system was very sensitive to the manner of capping so that great care was necessary to prevent the accumulation of trapped air beneath the cap and yet not change the effective level of the liquid by lowering the cap too far. There was also the previously mentioned problem of induced vibrations in the cap. Resonance was determined from the relative peak displacement amplitude as viewed on the oscilloscope. Identification of the bending mode was made from measured wall displacement phase changes using a stationary and circumferentially adjustable probe. An axial plot of the bending mode shapes also was

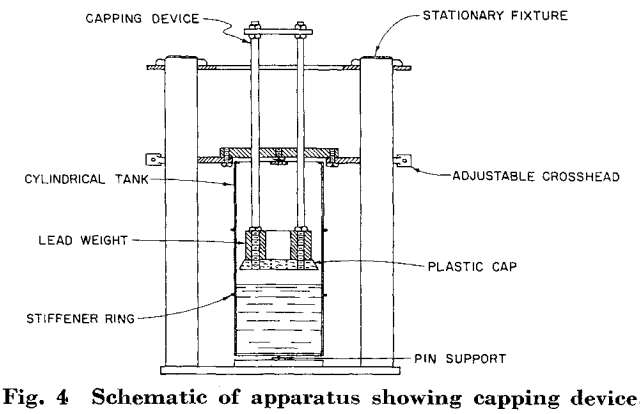

Fig. 4 Schematic of apparatus showing capping device.

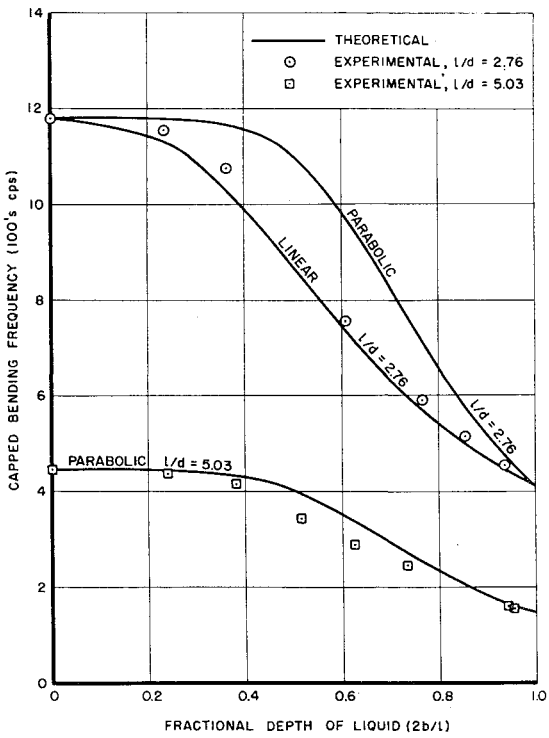

Fig. 5 Capped resonant bending frequency vs fractional liquid depth for two cantilever tanks.

made for correlation with those assumed in the theory. Water was the only liquid used for these tests.

Experimental Results and Discussion

Cantilever Tanks

Data were obtained for two cantilever tanks having l/d ratios of 2.76 and 5.03. These were chosen to lie in the region of maximum coupling effect (see Fig. 2). The third tank of $l/d = 1.41$ was found to be too short to obtain satisfactory bending data. Figure 5 shows the experimental and theoretical capped tank resonant frequencies as a function of the fractional depth of liquid in the tank. The theoretical uncoupled bending frequency is taken as

$$\omega_3 = [(\bar{m}_e\omega_e^2)/(\bar{m}_e + \bar{m}_{3,3})]^{1/2}$$

$\bar{m}_e\omega_e^2$ is the effective bending stiffness of the empty tank (the potential energy of the liquid due to bending is neglected in comparison with the elastic energy of the tank). $\bar{m}_e$ and $\bar{m}_{3,3}$ are the respective mass coefficients for the empty tank and the contained liquid. Because of the addition of the stiffener rings to the tanks it was necessary to adjust each theoretical empty tank frequency ω_e and mass $\bar{m}_e$. This was done by forcing these values to fit the experimental uncoupled, empty and full tank resonant frequencies.

The difference between the capped and uncapped resonant frequencies is plotted in Fig. 6 as the percentage frequency increase $[(\omega - \omega_3)/\omega_3] \times 100$ against fractional depth. For both the frequency and the frequency increase data, for the partially full tank, the agreement between experiment and the theory based on a parabolic mode shape is seen to diverge considerably. This raises the question as to whether or not the assumed mode shape is adequate to represent the actual conditions. For this reason the actual bending mode shapes for the two tanks were measured and are given in Fig. 7, along with the assumed parabolic curve. It is obvious that considerable divergence existed, being more pronounced for the tank of smaller l/d. The closer agreement between the mode shape for the tank of $l/d = 5.03$ and the parabola is reflected in the experimental results. Because of the high bending stiffness of the shorter tank, the mode shape shows little curvature.

In order to check whether or not the deviation between theory and experiment was primarily the result of the divergence from the assumed parabolic mode shape, the inertia coefficients for the liquid were recalculated for the case of $l/d = 2.76$ using a linear mode shape. The theoretical results for frequency and frequency increase based on the linear approximation are therefore also plotted in Figs. 5 and 6. The experimental data now were seen to fall between the linear and parabolic curves, as would be expected from the

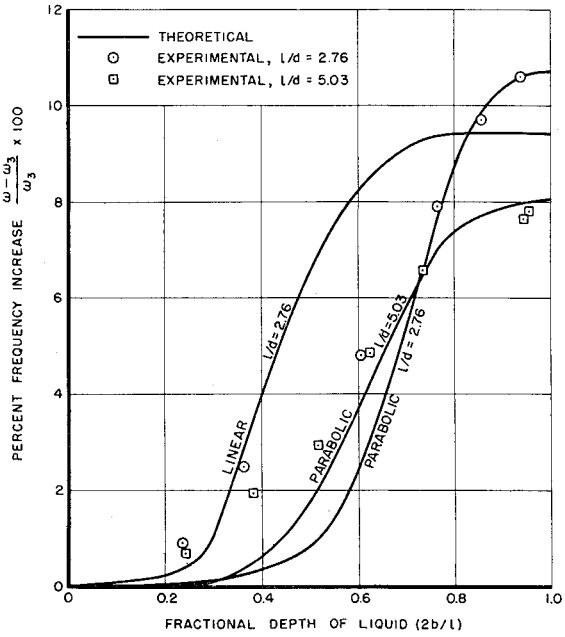

Fig. 6 Percent increase in resonant bending frequency vs fractional liquid depth for two cantilever tanks.

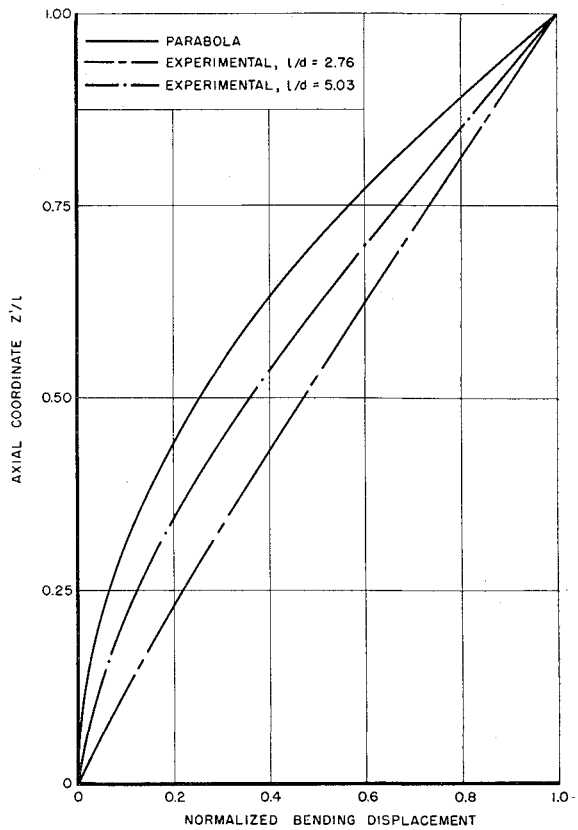

Fig. 7 Bending mode shapes for the two cantilever tanks.

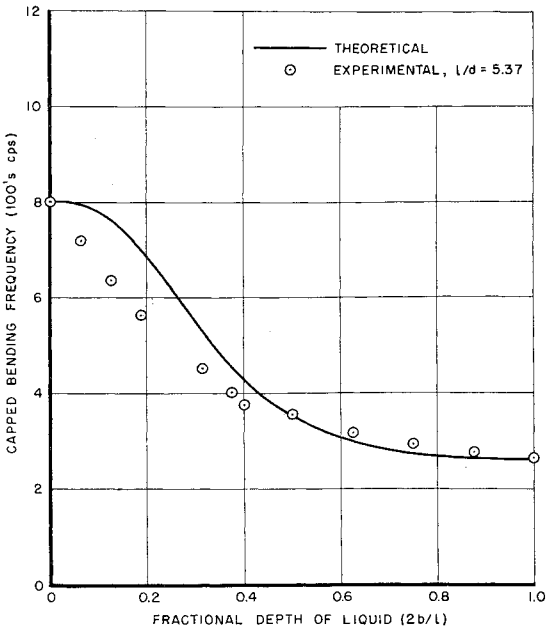

Fig. 8 Capped resonant bending frequency vs fractional liquid depth for the pin-ended tank.

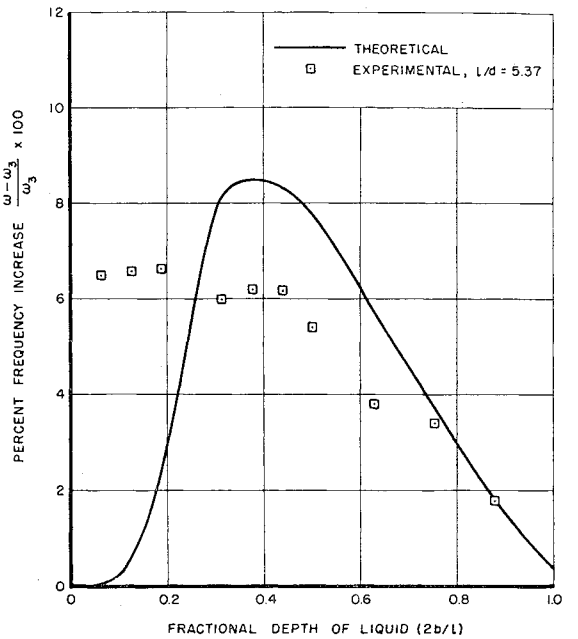

Fig. 9 Percent increase in resonant bending frequency vs fractional liquid depth for the pin-ended tank.

actual mode shape. Taking this sensitivity of the results to mode shape into account, the experimental points appear to correlate well with theory. In order to obtain more precise quantitative agreement, it would be necessary to use actual measured mode shapes, especially for the partially full tank where the mode shape is liable to change with changing depth. The change in mode shape for varying liquid depth was not pronounced in the cantilever tanks but will be seen to be significant for the pin-ended tanks.

Pin-Ended Tanks

Figures 8 and 9 show the capped tank bending resonant frequency and percent frequency shift vs fractional depth of liquid for a pin-ended tank of $l/d = 5.37$. It was not possible to obtain consistent bending data from the shorter tanks in the pin-ended configuration because of coupling with breathing resonances.

Figure 10 indicates that the mode shape problem is even more complicated for a pin-ended tank than for the cantilever tank. The full and empty tank mode shapes appear to be much like the half-sine wave assumed in the theory, but for the partially full tank considerable deviation is noted. It is difficult to make a direct comparison with the measured results because of the inaccuracy involved for this case in measuring the mode shape at the wall of the shell and not at its centerline. Rotation of the shell cross section near the ends causes the relative displacement of a point on the shell wall, as measured by the fixed, finite diameter, displacement transducer to be slightly different from that of a point at the same elevation on the centerline. This accounts for the apparent displacement of the bottom of the tank.[||] The evident and important conclusion, however, is that the mode shape continuously varies with depth of liquid in the tank. The maximum displacement occurs at the midpoint of the full shell, shifts downward until a depth of about $\frac{1}{4}$ full is reached, then shifts back upward until it again is at the midpoint for the empty shell. Since the bending frequencies are all highly sensitive to slight changes in mode shape, it is apparent that an exact solution would require accounting for the change of mode shape with depth, an extremely complex and mathematically cumbersome problem.

[||] In Fig. 10 the measured displacement at the top of the tank was set arbitrarily to zero for comparison with the assumed mode shape.

The theoretical curves of Figs. 8 and 9 are based on a half-sine wave mode shape, which is seen to be a good approximation for both the full and empty tank. At the lower fractional depths, where the deviation in mode shape is greatest, the experimental points also show the greatest deviation. The large deviations at very shallow depths, especially in the frequency shift, may be due partially to the fact that the cap on the liquid surface is fixed and does not rotate with the tank; this violates the theoretical assumption of the capped surface remaining normal to the generator of the

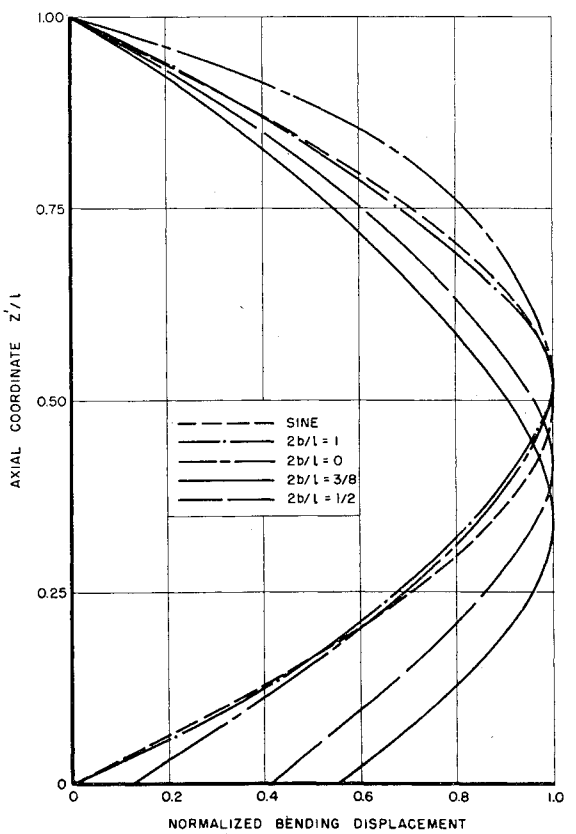

Fig. 10 Bending mode shapes for the pin-ended tank showing the effect of partial depth of liquid in the tank.

tank. For the pin-ended tank, where the bottom is free to rotate, this may become significant at very shallow depths because the end conditions predominate.

Conclusions

The presence of free liquid surface motion in a circular cylindrical tank always will increase the resonant bending frequency of the tank as compared with the tank having the same total mass of liquid but with the sloshing suppressed. Similarly, the resonant sloshing frequencies are decreased because of the coupling with bending, although not by a significant amount.

The increase in the coupled bending resonant frequency appears to be significant only for tanks where the effective sloshing mass is an appreciable part of the total vibrating mass, as in uniform cylindrical shells of small fineness ratio. Increases of up to 11% were observed experimentally in cantilever tanks and up to approximately 7% in pin-ended tanks. The experimental data presented for these two tank configurations conform, at least qualitatively, with the theory based on a Lagrangian formulation of the problem as first suggested by Miles and extended herein. In order to obtain more accurate quantitative agreement with theory, it would be necessary to consider a more accurate formulation of the bending mode shape. In the present work, a single mode approximation was made. It is possible within the framework of the theory to use the superposition of several tank modes in the formulation of the frequency determinant, thereby obtaining greater accuracy at the expense of computational effort. For the partially filled tank this becomes increasingly necessary as the mode shape may become quite unsymmetric at some depths. The added difficulty also arises that, for tanks of low fineness ratio (that region where the free surface boundary condition can have a significant effect on resonant frequency in bending), there also may exist many other resonant shell modes[1] at frequencies in the neighborhood of the bending mode. Thus, it may become necessary to consider these modes in certain cases. An analysis of the effect of the free surface on the resonant frequencies of these shell modes has been given in a recent report by Lianis and Fontenot.[7]

For tanks of low bending frequency resulting from masses added to the system, as in space vehicle booster tanks with engines and upper stages attached, the contribution of the sloshing mass to the total vibrating mass may become negligible in calculating resonant bending frequencies.

Appendix A

The kinetic and potential energy coefficients m_{ij} and k_{ij} for the tank subject to coupled bending and liquid oscillations as shown in Fig. 1 are given below. These are essentially the same as those as given by Miles.[2] Following Miles, $i = 3$ corresponds to a bending displacement along $\theta = 0$, and $i = s + 3$ corresponds to a displacement of the free liquid surface from a plane normal to the axis of the tank. The bars over the coefficients indicate normalization by the total liquid mass, $M = 2\pi a^2 b \rho_L$.

$$\bar{m}_{3,3} = F_0^2 + \frac{1}{2}\sum_{s=1}^{\infty} \psi_s F_s^2 + \frac{a^2}{b}\sum_{s=1}^{\infty} \frac{f'(-b)x_s(-b) - f'(b)x_s(b)}{\beta_s^2 - 1} + \frac{1}{8}\frac{a^2}{b}[f'(-b) - f'(b)]F_0 + \frac{2b}{\pi^2}\sum_{s=1}^{\infty}\frac{1-\psi_s}{s^2} \times [(-1)^{s+1}f'(b) + f'(-b)]F_s + \frac{a^3}{b}\sum_{s=1}^{\infty}\frac{\operatorname{csch}(2\beta_s b/a)}{\beta_s^3(\beta_s^2-1)^{-1}} \times \left\{[f'^2(b) + f'^2(-b)]\cosh\left(\frac{2\beta_s b}{a}\right) - 2f'(b)f'(-b)\right\}$$

$$\bar{m}_{3,s+3} = \frac{a}{2b}x_s(b) - \frac{a^2}{2b\beta_s^3}\operatorname{csch}\left(\frac{2\beta_s b}{a}\right) \times \left[f'(b)\cosh\left(\frac{2\beta_s b}{a}\right) - f'(-b)\right]$$

$$\bar{m}_{s+3,s+3} = \frac{a}{4b}\frac{\beta_s^2 - 1}{\beta_s^3}\coth\left(\frac{2\beta_s b}{a}\right)$$

$$\bar{m}_e = \frac{M_e}{M}\left[\bar{f}^2(z') + \frac{a^2}{2}\bar{f}'^2(z')\right]^{\#}$$

$$\bar{f}^2(z') = \frac{1}{l}\int_0^l f^2(z')dz'$$

$$\bar{k}_{3,3} = g\left\{\frac{a^2}{8b}[f'^2(b) - f'^2(-b)] + \frac{1}{2b}\int_{-b}^{b} zf'^2(z)dz - \frac{1}{2}\int_{z_0}^{b} f'^2(z)dz + \frac{1}{2}\int_{-b}^{z_0} f'^2(z)dz\right\}$$

$$\bar{k}_{3,s+3} = -\frac{ga}{2b\beta_s^2}f'(b)$$

The following notation has been used:

$$F_0 = \frac{1}{2b}\int_{-b}^{b} f(z)dz$$

$$F_s = \frac{1}{b}\int_{-b}^{b} f(z)\cos\left[\frac{s\pi(z+b)}{2b}\right]dz \qquad s \geq 1$$

$$\psi_s = \frac{I_1(s\pi a/2b)}{(s\pi a/2b)I_0(s\pi a/2b) - I_1(s\pi a/2b)}$$

$$x_s(b) = \frac{\operatorname{csch}(2\beta_s b/a)}{\beta_s a}\int_{-b}^{b} f(z)\cosh\left[\frac{\beta_s(z+b)}{a}\right]dz$$

$$J_1'(\beta_s) = 0$$

Appendix B

The m_{ij},k_{ij}, and assumed bending mode shapes for the particular tank configurations studied in this paper are given below.

Cantilever Tank

$$f(z) = \left(\frac{z+b}{l}\right)^2 = \left(\frac{z'}{l}\right)^2$$

$$\bar{m}_{3,3} = \left(\frac{2b}{l}\right)^4\left[\frac{1}{45} - \frac{1}{6}\left(\frac{a}{b}\right)^2 - \frac{7}{384}\left(\frac{a}{b}\right)^4 + \frac{16}{\pi^4}\sum_{s=1}^{\infty}\frac{\psi_s}{s^4} + 2\left(\frac{a}{b}\right)^3\sum_{s=1}^{\infty}\frac{\coth(2\beta_s b/a)}{\beta_s^3(\beta_s^2-1)}\right]$$

$$\bar{m}_{3,s+3} = \left(\frac{2b}{l}\right)^2\left[\frac{1}{2\beta_s^2}\left(\frac{a}{b}\right) - \left(\frac{a}{b}\right)^2 \times \frac{\coth(2\beta_s b/a)}{\beta_s^3} + \frac{1}{4\beta_s^4}\left(\frac{a}{b}\right)^3\right]$$

$$\bar{m}_{s+3,s+3} = \frac{1}{4}\left(\frac{a}{b}\right)\frac{(\beta_s^2-1)}{\beta_s^3}\coth\left(\frac{2\beta_s b}{a}\right)$$

$$\bar{m}_e = \frac{t\rho_s}{b\rho_L}\left[\frac{1}{5}\left(\frac{l}{b}\right)\left(\frac{b}{a}\right) + \frac{2}{3}\left(\frac{a}{b}\right)\left(\frac{b}{l}\right)\right]$$

$$\bar{k}_{3,3} = \frac{2g}{l}\left[\left(\frac{b}{l}\right)\left(\frac{a}{l}\right)^2 - \frac{4}{3}\left(\frac{b}{l}\right)^3\right]$$

$$\bar{k}_{3,s+3} = -\frac{2g}{l\beta_s^2}\left(\frac{a}{l}\right)$$

The second term in the brackets includes the effect of rotary inertia of the tank walls not included in Ref. 2. M_e is the total tank mass.

Pin-Ended Tank

Mode shape

$$f(z) = \sin\left(\frac{\pi(z+b)}{l}\right) = \sin\frac{\pi z'}{l}$$

$$\bar{m}_{3,3} = \left[\frac{1}{4\pi^2}\left(\frac{l}{b}\right)^2 + \frac{1}{16}\left(\frac{a}{b}\right)^2\right]\left[1 - \cos\left(\frac{2\pi b}{l}\right)\right]^2 + \sum_{s=1}^{\infty}\frac{2}{\pi^2 s^2} \times \frac{[1+(-1)^{s+1}\cos(2\pi b/l)]^2}{[1-(sl/2b)^2]} \times \left\{1 - \psi_s\left[\frac{(2b/sl)^2-2}{(2b/sl)^2-1}\right]\right\} + \sum_{s=1}^{\infty}\frac{a/b}{\beta_s(\beta_s^2-1)} \times \left[\frac{(\pi a/\beta_s l)^2+2}{(\beta_s l/\pi a)^2+1}\right]\left\{\coth\left(\frac{2\beta_s b}{a}\right)\left[1+\cos^2\left(\frac{2\pi b}{l}\right)\right] - 2\cos\left(\frac{2\pi b}{l}\right)\operatorname{csch}\left(\frac{2\beta_s b}{a}\right)\right\} - \sum_{s=1}^{\infty}\frac{1}{2\pi(\beta_s^2-1)} \times \frac{\sin(4\pi b/l)}{(b/l)+(\beta_s b/\pi a)^2(l/a)}$$

$$\bar{m}_{3,s+3} = \frac{(l/b)}{2\pi[1+(\beta_s l/\pi a)^2]}\left\{\frac{1}{\beta_s}\left[2+\left(\frac{\pi a}{\beta_s l}\right)^2\right] \times \left[\operatorname{csch}\left(\frac{2\beta_s b}{a}\right) - \cos\left(\frac{2\pi b}{l}\right)\coth\left(\frac{2\beta_s b}{a}\right)\right] + \frac{1}{\pi}\left(\frac{l}{a}\right)\sin\left(\frac{2\pi b}{l}\right)\right\}$$

$$\bar{m}_{s+3,s+3} = \frac{a}{4b}\,\frac{(\beta_s^2-1)}{\beta_s^3}\coth\left(\frac{2\beta_s b}{a}\right)$$

$$\bar{k}_{3,3} = \frac{g}{16b}\left\{-\frac{8\pi^2 b^2}{l^2} + \left(\frac{\pi^2 a^2}{l^2}+1\right)\left[\cos\left(\frac{4\pi b}{l}\right)-1\right]\right\}$$

$$\bar{k}_{3,s+3} = -\frac{\pi g a}{2bl\beta_s^2}\cos\left(\frac{2\pi b}{l}\right)$$

$$\bar{m}_e = \frac{tl\rho_s}{2ba\rho_L}\left[1+\frac{\pi^2}{2}\left(\frac{a}{l}\right)^2\right]$$

References

[1] Lindholm, U. S., Kana, D. D., and Abramson, H. N., "Breathing vibrations of a circular cylindrical shell with an internal liquid," J. Aerospace Sci. 29, 1052–1059 (1962).

[2] Miles, J. W., "On the sloshing of liquid in a flexible tank," J. Appl. Mech. 25, 277–283 (1958).

[3] Reissner, E., "Notes on the forced and free vibrations of pressurized cylindrical shells which contain a heavy liquid with a free surface," AM 6-15, GMTR 87, Space Technology Lab. Inc., Los Angeles, Calif. (November 1956).

[4] Rabinovich, F. I., "Concerning the equations of elastic oscillations of thin-walled bars filled with a liquid having a free surface," Space Technology Lab., transl. STL-T-RV-19 (June 1960) from Akad. Nauk SSR Izv. Otd. Tekhn. Nauk Mekhan. i Machinostr., no. 4 (1959).

[5] Bauer, H. F., "Fluid oscillations in a circular cylindrical tank due to bending of the tank wall," Rept. DA-TR-3-58, Redstone Arsenal, Ala. (April 1958).

[6] Bauer, H. F., "Damped fluid oscillations in a circular cylindrical tank due to bending of the tank wall," Rept. DA-TR-9-58, Army Ballistic Missile Agency, Redstone Arsenal, Ala. (May 1958).

[7] Lianis, G. and Fontenot, L. L., "Analysis of the free vibrations of pressurized cylindrical shells filled with an ideal liquid having a free surface," General Dynamics/Astronautics Rept. ERR-AN-194 (September 1962).

SEPTEMBER 1963 AIAA JOURNAL VOL. 1, NO. 9

Response of Elastic Columns to Axial Pulse Loading

NORRIS J. HUFFINGTON JR.*

Martin Company, Baltimore, Md.

In the analysis of columns subjected to axial load pulses of short duration, the nonuniform distribution of longitudinal force along the axis has a significant effect upon the solution. Consequently, it is important to employ a formulation that properly accounts for the propagation of longitudinal and flexural waves and for their interaction. The equations of motion are simultaneous nonlinear partial differential equations. These are solved by an explicit finite difference procedure, taking into account the requirements for stability of the numerical analysis. Solutions are contrasted for two theories, in one of which the effects of rotatory inertia and transverse shear deformation are incorporated, whereas in the other these are omitted. A limited study of the effects of varying system parameters is also presented. For the problems treated, the induced flexural stresses are found to remain small in comparison to the axial stresses.

Introduction

THE topic of columns subjected to time-varying axial loads has been considered by many investigators dating back at least to the 1933 paper by Koning and Taub.[1] Much of the literature prior to 1958 has been summarized in a report by Kotowski.[2] For the most part, investigators in this era chose to neglect the effect of longitudinal inertia. This is equivalent to assuming that axial stress waves can be propagated with infinite velocity so that there can be no variation in axial force along the column. For axial forces that vary with a frequency much less than the fundamental frequency of longitudinal vibration, neglect of longitudinal inertia should constitute a satisfactory engineering approximation. Additionally, the paper by Gerard and Becker[3] and the report by Hoppmann[4] should be noted in which the effects of longitudinal waves were considered. However, in both instances the transverse inertia forces were omitted, providing a basis for doubts regarding the physical correspondence of these formulations.

Received April 4, 1963; revision received July 15, 1963.

* Chief, Dynamics Research.